First test of Lorentz violation with a reactor-based antineutrino experiment

Y. Abe,[27] C. Aberle,[21] J. C. dos Anjos,[5] M. Bergevin,[9] A. Bernstein,[16] T. J. C. Bezerra,[29] L. Bezrukhov,[14] E. Blucher,[6] N. S. Bowden,[16] C. Buck,[21] J. Busenitz,[2] A. Cabrera,[4] E. Caden,[10] L. Camilleri,[8] R. Carr,[8] M. Cerrada,[7] P.-J. Chang,[17] P. Chimenti,[33] T. Classen,[9,16] A. P. Collin,[15] E. Conover,[6] J. M. Conrad,[20] J. I. Crespo-Anadón,[7] K. Crum,[6] A. Cucoanes,[25,15] M. V. D'Agostino,[3] E. Damon,[10] J. V. Dawson,[4,35] S. Dazeley,[16] D. Dietrich,[32] Z. Djurcic,[3] M. Dracos,[24] V. Durand,[15,4] J. Ebert,[26] Y. Efremenko,[26] M. Elnimr,[25] A. Erickson,[16] M. Fallot,[25] M. Fechner,[15] F. von Feilitzsch,[30] J. Felde,[9] V. Fischer,[15] D. Franco,[4] A. J. Franke,[8] M. Franke,[30] H. Furuta,[29] R. Gama,[5] I. Gil-Botella,[7] L. Giot,[25] M. Göger-Neff,[30] L. F. G. Gonzalez,[34] M. C. Goodman,[3] J. TM. Goon,[2] D. Greiner,[32] N. Haag,[30] S. Habib,[2] C. Hagner,[11] T. Hara,[18] F. X. Hartmann,[21] J. Haser,[21] A. Hatzikoutelis,[26] T. Hayakawa,[22,15] M. Hofmann,[30] G. A. Horton-Smith,[17] M. Ishitsuka,[27] J. Jochum,[32] C. Jollet,[24] C. L. Jones,[20] F. Kaether,[21] L. N. Kalousis,[36] Y. Kamyshkov,[26] D. M. Kaplan,[13] T. Katori,[20] T. Kawasaki,[22] G. Keefer,[16] E. Kemp,[34] H. de Kerret,[4,35] T. Konno,[27] D. Kryn,[4] M. Kuze,[27] T. Lachenmaier,[32] C. E. Lane,[10] T. Lasserre,[15,4] A. Letourneau,[15] D. Lhuillier,[15] H. P. Lima, Jr.,[5] M. Lindner,[21] J. M. López-Castaño,[7] J. M. LoSecco,[23] B. K. Lubsandorzhiev,[14] S. Lucht,[1] D. McKee,[17] J. Maeda,[28] C. N. Maesano,[9] C. Mariani,[36] J. Maricic,[10] J. Martino,[25] T. Matsubara,[28] G. Mention,[15] A. Meregaglia,[24] M. Meyer,[11] T. Miletic,[10] R. Milincic,[10] H. Miyata,[22] Th. A. Mueller,[15,29] Y. Nagasaka,[12] K. Nakajima,[22] P. Novella,[7] M. Obolensky,[4] L. Oberauer,[30] A. Onillon,[25] A. Osborn,[26] I. Ostrovskiy,[2] C. Palomares,[7] I. M. Pepe,[5] S. Perasso,[10] P. Perrin,[15] P. Pfahler,[30] A. Porta,[25] W. Potzel,[30] G. Pronost,[25] J. Reichenbacher,[2] B. Reinhold,[21] A. Remoto,[25,4] M. Röhling,[32] R. Roncin,[4] S. Roth,[1] B. Rybolt,[26] Y. Sakamoto,[31] R. Santorelli,[7] F. Sato,[28] S. Schönert,[30] S. Schoppmann,[1] T. Schwetz,[21] M. H. Shaevitz,[8] D. Shrestha,[17] J-L. Sida,[15] V. Sinev,[14,15] M. Skorokhvatov,[19] E. Smith,[10] J. Spitz,[20] A. Stahl,[1] I. Stancu,[2] L. F. F. Stokes,[32] M. Strait,[6] A. Stüken,[1] F. Suekane,[29] S. Sukhotin,[19] T. Sumiyoshi,[28] Y. Sun,[2] K. Terao,[20] A. Tonazzo,[4] M. Toups,[8] H. H. Trinh Thi,[30] G. Valdiviesso,[34] C. Veyssiere,[15] S. Wagner,[21] H. Watanabe,[21] B. White,[26] C. Wiebusch,[1] L. Winslow,[20] M. Worcester,[6] M. Wurm,[11] E. Yanovitch,[14] F. Yermia,[25] and V. Zimmer[30]

(Double Chooz Collaboration)

[1]*III. Physikalisches Institut, RWTH Aachen University, Aachen 52056, Germany*
[2]*Department of Physics and Astronomy, University of Alabama, Tuscaloosa, Alabama 35487, USA*
[3]*Argonne National Laboratory, Argonne, Illinois 60439, USA*
[4]*APC, AstroParticule et Cosmologie, Université Paris Diderot, CNRS/IN2P3, CEA/IRFU, Observatoire de Paris, Sorbonne Paris Cité 75205, Paris Cedex 13, France*
[5]*Centro Brasileiro de Pesquisas Físicas, Rio de Janeiro, Rio de Janeiro, cep 22290-180, Brazil*
[6]*The Enrico Fermi Institute, The University of Chicago, Chicago, Illinois 60637, USA*
[7]*Centro de Investigaciones Energéticas, Medioambientales y Tecnológicas, CIEMAT E-28040, Madrid, Spain*
[8]*Columbia University, New York, New York 10027, USA*
[9]*University of California, Davis, California 95616-8677, USA*
[10]*Physics Department, Drexel University, Philadelphia, Pennsylvania 19104, USA*
[11]*Institut für Experimentalphysik, Universität Hamburg, 22761 Hamburg, Germany*
[12]*Hiroshima Institute of Technology, Hiroshima 731-5193, Japan*
[13]*Department of Physics, Illinois Institute of Technology, Chicago, Illinois 60616, USA*
[14]*Institute of Nuclear Research of the Russian Academy of Science, Moscow 117312, Russia*
[15]*Commissariat à l'Energie Atomique et aux Energies Alternatives, Centre de Saclay, IRFU 91191 Gif-sur-Yvette, France*
[16]*Lawrence Livermore National Laboratory, Livermore, California 94550, USA*
[17]*Department of Physics, Kansas State University, Manhattan, Kansas 66506, USA*
[18]*Department of Physics, Kobe University, Kobe 657-8501, Japan*
[19]*NRC Kurchatov Institute , Moscow 123182, Russia*
[20]*Massachusetts Institute of Technology, Cambridge, Massachusetts 02139, USA*
[21]*Max-Planck-Institut für Kernphysik, Heidelberg 69117, Germany*
[22]*Department of Physics, Niigata University, Niigata 950-2181, Japan*
[23]*University of Notre Dame, Notre Dame, Indiana 46556-5670, USA*
[24]*IPHC, Université de Strasbourg, CNRS/IN2P3 F-67037 Strasbourg, France*
[25]*SUBATECH, CNRS/IN2P3, Université de Nantes, Ecole des Mines de Nantes F-44307 Nantes, France*
[26]*Department of Physics and Astronomy, University of Tennessee, Knoxville, Tennessee 37996, USA*
[27]*Department of Physics, Tokyo Institute of Technology, Tokyo 152-8551, Japan*

[28]*Department of Physics, Tokyo Metropolitan University, Tokyo 192-0397, Japan*
[29]*Research Center for Neutrino Science, Tohoku University, Sendai 980-8578, Japan*
[30]*Physik Department, Technische Universität München, Garching 85747, Germany*
[31]*Tohoku Gakuin University, Sendai 981-3193, Japan*
[32]*Kepler Center for Astro and Particle Physics, Universität Tübingen, Tübingen 72076, Germany*
[33]*Universidade Federal do ABC, UFABC, Sao Paulo, Santo André, São Paulo, Brazil*
[34]*Universidade Estadual de Campinas-UNICAMP, Campinas, São Paulo, Brazil*
[35]*Laboratoire Neutrino de Champagne Ardenne, domaine d'Aviette 08600 Rancennes, France*
[36]*Center for Neutrino Physics, Virginia Tech, Blacksburg, Virginia 24061, USA*
(Received 26 September 2012; published 28 December 2012)

We present a search for Lorentz violation with 8249 candidate electron antineutrino events taken by the Double Chooz experiment in 227.9 live days of running. This analysis, featuring a search for a sidereal time dependence of the events, is the first test of Lorentz invariance using a reactor-based antineutrino source. No sidereal variation is present in the data and the disappearance results are consistent with sidereal time independent oscillations. Under the Standard-Model Extension, we set the first limits on 14 Lorentz violating coefficients associated with transitions between electron and tau flavor, and set two competitive limits associated with transitions between electron and muon flavor.

Recently, we reported evidence of electron antineutrino disappearance with the Double Chooz far detector, 1050 m away from two 4.25 GW reactor cores [1,2], which generally is interpreted in terms of mass-induced neutrino oscillations. A path to more exotic physics beyond the Standard Model (SM) may be gained by carefully examining the oscillation behavior. In particular, the collected electron antineutrino sample also provides an opportunity to search for the violation of Lorentz invariance.

Lorentz invariance requires that the behavior of a particle is independent of its direction or boost velocity. The as-yet-unseen violation of this principle is predicted to occur at the Planck scale and is especially interesting as it can occur dynamically via spontaneous Lorentz symmetry breaking [3]. The process of neutrino oscillation, in which a neutrino of one flavor transforms into another flavor after traveling a distance, is due to interference between the slightly different Hamiltonian eigenstates of the propagating particle. The experimental observable, oscillation probability, is therefore quite sensitive to small couplings between neutrinos and a possible Lorentz violating field.

Testing Lorentz violation with the natural interferometer of neutrino oscillation has been done in several experiments, including MINOS [4], IceCube [5], LSND [6], and MiniBooNE [7]. These tests all fall under the formalism of a search within the Standard-Model Extension (SME) [8]. In this paper, we describe the first search for Lorentz violation using reactor antineutrinos.

In the SME, all possible types of Lorentz violation are added to the SM Lagrangian. Here, we limit ourselves to the renormalizable sector (referred to as the minimal SME). For Lorentz violating neutrino oscillation, the effective Hamiltonian is written as [9]

$$(h^{\nu}_{\text{eff}})_{ab} \sim \frac{(m^2)_{ab}}{2E} + \frac{1}{E}[(a_L)^{\mu}p_{\mu} - (c_L)^{\mu\nu}p_{\mu}p_{\nu}]_{ab}, \quad (1)$$

where E and p_{μ} are the energy and 4-momentum of the neutrino and $(m^2)_{ab}$ refers to the neutrino mass in the flavor basis represented by a and b. The *CPT*-odd coefficient $(a_L)^{\mu}_{ab}$ switches sign for antineutrinos and violates both Lorentz and *CPT* symmetry, while the *CPT*-even coefficient $(c_L)^{\mu\nu}_{ab}$ violates Lorentz but maintains *CPT*. Both are vector and tensor and consist of direction independent parts $[(a_L)^T_{ab}, (a_L)^Z_{ab}, (c_L)^{TT}_{ab}, (c_L)^{TZ}_{ab},$ and $(c_L)^{ZZ}_{ab}]$ and direction dependent parts $[(a_L)^X_{ab}, (a_L)^Y_{ab}, (c_L)^{TX}_{ab}, (c_L)^{TY}_{ab}, (c_L)^{XX}_{ab}, (c_L)^{XY}_{ab}, (c_L)^{XZ}_{ab}, (c_L)^{YY}_{ab},$ and $(c_L)^{YZ}_{ab}]$ in the Sun-centered coordinate system (represented by the superscripts). A measured nonzero direction dependent component would be clear evidence of an anisotropy in the Universe and Lorentz violation. As discussed later, no evidence for Lorentz violation has been found and our goal is therefore to set limits on these coefficients. We note that the known neutrino mass term in the flavor basis in this formalism is neglected in order to follow a conservative approach when setting these limits.

Sidereal time is based on the Earth's orientation relative to the fixed stars. The unambiguous signature of Lorentz violation is a sidereal modulation of an experimental observable such as neutrino oscillation probability. A sidereal variation is expected for an experiment moving in a fixed Lorentz violating field with the rotation of the Earth. We probe this field by searching for such a dependence among the collected electron antineutrino events. The antineutrino vector is set using the antineutrino source and the location of the detector. The location of the source is taken to be a weighted point in between the two cores, 6° apart relative to the detector, representative of the number of antineutrinos expected from each during the physics run.

The data set used for this analysis was obtained with the Double Chooz experiment between April 13, 2011 and March 15, 2012. Electron antineutrinos interact in the detector via the inverse beta decay (IBD) process, $\bar{\nu}_e + p \rightarrow e^+ + n$. IBD events produce a distinct double coincidence signature from the prompt positron signal followed by neutron capture 30 μs (mean time) later. The "inner detector," composed of three concentric cylindrical regions separated by acrylic, is used to observe and efficiently reconstruct these events as well as mitigate background. The innermost 10 m^3 cylinder contains 1 g/l gadolinium-doped scintillator and forms the antineutrino target. Surrounding this is the "gamma catcher" designed to detect gamma rays escaping the target volume. The gamma catcher volume is then enveloped by a nonscintillating oil buffer in which 390 10-inch PMTs are immersed. The inner detector is surrounded by a steel vessel that forms an optically isolated outer cylinder filled with scintillator. This "inner veto," along with an "outer veto" mounted above it and 15 cm of shielding steel, is used to reject cosmic ray events.

The antineutrino sample and event selection criteria are identical to those used for the disappearance analysis reported in Ref. [2]. The data consist of 8249 IBD candidates collected with 227.9 live days and 33.7 GW-ton-years exposure. There are 497 background events expected in this sample. The background is mainly composed of (1) cosmogenic radioisotopes, such as ^{8}He and ^{9}Li, which decay via the emission of βn, (2) cosmogenic stopping muons as well as fast neutrons that interact multiple times in the inner detector, and (3) accidental coincidence of a radioactivity-induced prompt signal followed by a neutronlike signal. Background event rate as a function of sidereal time is treated as a constant. As the dominant background contributions to the Double Chooz analyses arise as the result of cosmic ray muons, we study the time dependence of muon veto rate in order to justify this assumption. The maximum variation in muon veto rate as a function of sidereal time is about 0.5%. A background variation in time at this level would create a maximum variation in disappearance probability of $\sim$0.03%.

The background-subtracted IBD candidate sample is directly compared to the Monte Carlo (MC) expectation in order to probe a possible sidereal time dependence. The unoscillated MC expectation is based on the IBD cross section, the reactor flux prediction, the detector response, and the number of protons in the detection volume. The expectation is formed from each of these variables on a run-by-run basis, with each physics run lasting approximately one hour. We note that the thermal power of each core is estimated in <1-minute time intervals and the uncertainty on the total power is 0.5%. The reactor flux prediction uses extensive input from the Chooz reactor facility and Électricité de France (EDF). The quality of the code has been benchmarked [10] and compared to EDF

assembly simulations. The $\bar{\nu}_e$ spectrum is taken directly from Refs. [11,12] and is normalized to the Bugey4 rate measurement [13]. The analysis input information, shown in Fig. 1, is assigned to one of 24 bins between 0 and 23.934 hours (one sidereal day). A MC expectation event weight is split up between the relevant time bins based on the time and length of the run while a data event is placed in a bin based on its DAQ time stamp.

A number of sources of systematic uncertainty are considered. These include those associated with the background prediction, the detector and detector response, and the reactor flux (normalization and shape). The reactor flux and detector operations are both weak functions of solar time due to human activity as the cores turned on/off multiple times during the run and detector calibrations are generally done during the daylight hours. Day-night effects are well accounted for in the MC prediction. All uncertainties are included in a covariance matrix, fully describing the predicted statistical and systematic errors. The 3.93 minute/day difference between sidereal and solar time, compounded over the $\sim$1-year physics run, largely removes any potential for an unaccounted modulation in sidereal time associated with small modulations related to solar dependence. The detector and background prediction uncertainties are considered uncorrelated with each other and fully correlated in sidereal time. A thorough explanation of the various uncertainties and their determination can be found in Ref. [2], noting that correlations in time (as opposed to antineutrino energy in the reference) are most important here. The total fractional uncertainty with respect to the MC expectation is 2.9%. The statistical uncertainty contributes at the level of 1.1% and systematic uncertainties are led by the reactor flux and detector response (1.7%) and the background prediction (1.7%).

In the three active flavor neutrino oscillation framework, the $\bar{\nu}_e \rightarrow \bar{\nu}_e$ probability can be written as a function of $\bar{\nu}_e \rightarrow \bar{\nu}_\mu$ and $\bar{\nu}_e \rightarrow \bar{\nu}_\tau$ ($P_{\bar{\nu}_e \rightarrow \bar{\nu}_e} = 1 - P_{\bar{\nu}_e \rightarrow \bar{\nu}_\mu} - P_{\bar{\nu}_e \rightarrow \bar{\nu}_\tau}$). Under the SME, both $P_{\bar{\nu}_e \rightarrow \bar{\nu}_\mu}$ and $P_{\bar{\nu}_e \rightarrow \bar{\nu}_\tau}$ are written as functions of five free parameters [14]:
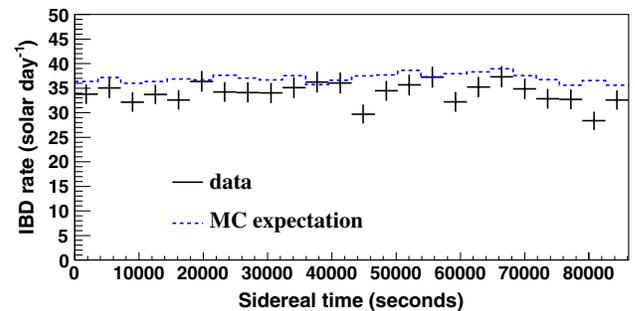

FIG. 1 (color online). The background subtracted data and MC expectation IBD event rates as a function of sidereal time. The MC expectation assumes no antineutrino disappearance. Total errors (statistical and systematic) are shown on the data points.

$$P_{\bar{\nu}_e \to \bar{\nu}_e} \simeq 1 - \frac{|(h_{\text{eff}})_{\bar{e}\bar{\mu}}|^2 L^2}{(\hbar c)^2} - \frac{|(h_{\text{eff}})_{\bar{e}\bar{\tau}}|^2 L^2}{(\hbar c)^2}$$

$$= 1 - \frac{L^2}{(\hbar c)^2}[|(\mathcal{C})_{\bar{e}\bar{\mu}} + (\mathcal{A}_s)_{\bar{e}\bar{\mu}}\sin\omega_\oplus T_\oplus + (\mathcal{A}_c)_{\bar{e}\bar{\mu}}\cos\omega_\oplus T_\oplus + (\mathcal{B}_s)_{\bar{e}\bar{\mu}}\sin 2\omega_\oplus T_\oplus + (\mathcal{B}_c)_{\bar{e}\bar{\mu}}\cos 2\omega_\oplus T_\oplus|^2 + |(\mathcal{C})_{\bar{e}\bar{\tau}}$$

$$+ (\mathcal{A}_s)_{\bar{e}\bar{\tau}}\sin\omega_\oplus T_\oplus + (\mathcal{A}_c)_{\bar{e}\bar{\tau}}\cos\omega_\oplus T_\oplus + (\mathcal{B}_s)_{\bar{e}\bar{\tau}}\sin 2\omega_\oplus T_\oplus + (\mathcal{B}_c)_{\bar{e}\bar{\tau}}\cos 2\omega_\oplus T_\oplus|^2]. \tag{2}$$

The disappearance probability is a function of sidereal time $T_\oplus$, sidereal frequency $\omega_\oplus$ $[2\pi/86164.1 \frac{\text{rad}}{\text{s}}]$, baseline L, and ten amplitudes (parameters). The parameters themselves are composed of the Lorentz violating coefficients introduced in Eq. (1), antineutrino energy, and the antineutrino-source-to-detector vector. We aim to reduce this equation since there are too many parameters for a realistic fit and measurement extraction. Ideally, this reduction proceeds without any assumptions in a model independent way.

Double Chooz's maximum sensitivity to the *CPT*-odd and *CPT*-even SME coefficients is on the order of $\sim 10^{-20}$ GeV and $\sim 10^{-18}$, respectively, determined by considering the maximum oscillation condition in the effective Hamiltonian [Eq. (1)]. Noting that the effective Hamiltonian is Hermitian and μ-e results can be applied to e-μ, the MINOS near detector [4] and MiniBooNE [7] measurements both place significantly better limits on all *CPT*-even coefficients at the level of $\sim 10^{-21}$ and $\sim 10^{-20}$, respectively. The ten relevant SME coefficients are therefore set to zero, corresponding to the removal of two parameters, $(\mathcal{B}_s)_{\bar{e}\bar{\mu}}$ and $(\mathcal{B}_c)_{\bar{e}\bar{\mu}}$, from Eq. (2). It is now difficult to remove more parameters in a model independent way and we cannot reduce Eq. (2) further using existing measurements. We therefore study two different sets of assumptions.

The assumption that all Lorentz violating oscillations occur in electron antineutrino to tau antineutrino transitions $(P_{\bar{\nu}_e \to \bar{\nu}_\mu} = 0, P_{\bar{\nu}_e \to \bar{\nu}_\tau} \neq 0)$ is studied with the "e-τ fit":

$$P_{\bar{\nu}_e \to \bar{\nu}_e} \simeq 1 - \frac{L^2}{(\hbar c)^2}[|(\mathcal{C})_{\bar{e}\bar{\tau}} + (\mathcal{A}_s)_{\bar{e}\bar{\tau}}\sin\omega_\oplus T_\oplus$$
$$+ (\mathcal{A}_c)_{\bar{e}\bar{\tau}}\cos\omega_\oplus T_\oplus + (\mathcal{B}_s)_{\bar{e}\bar{\tau}}\sin 2\omega_\oplus T_\oplus$$
$$+ (\mathcal{B}_c)_{\bar{e}\bar{\tau}}\cos 2\omega_\oplus T_\oplus|^2]. \tag{3}$$

The five free parameters $[(\mathcal{C})_{\bar{e}\bar{\tau}}, (\mathcal{A}_s)_{\bar{e}\bar{\tau}}, (\mathcal{A}_c)_{\bar{e}\bar{\tau}}, (\mathcal{B}_s)_{\bar{e}\bar{\tau}}$, and $(\mathcal{B}_c)_{\bar{e}\bar{\tau}}]$ themselves contain 14 of the e-τ sector SME coefficients introduced in Eq. (1).

The second model is based on the assumption that all Lorentz violating oscillations occur in electron antineutrino to muon antineutrino transitions $(P_{\bar{\nu}_e \to \bar{\nu}_\mu} \neq 0, P_{\bar{\nu}_e \to \bar{\nu}_\tau} = 0)$ and is referred to as the "e-μ fit":

$$P_{\bar{\nu}_e \to \bar{\nu}_e} \simeq 1 - \frac{L^2}{(\hbar c)^2}[|(\mathcal{C})_{\bar{e}\bar{\mu}} + (\mathcal{A}_s)_{\bar{e}\bar{\mu}}\sin\omega_\oplus T_\oplus$$
$$+ (\mathcal{A}_c)_{\bar{e}\bar{\mu}}\cos\omega_\oplus T_\oplus|^2]. \tag{4}$$

This equation has only three free parameters $[(\mathcal{C})_{\bar{e}\bar{\mu}}, (\mathcal{A}_s)_{\bar{e}\bar{\mu}}$, and $(\mathcal{A}_c)_{\bar{e}\bar{\mu}}]$, as the MINOS and MiniBooNE constraints have removed the *CPT*-even coefficients, and contains four e-μ sector SME coefficients. The $\mathcal{C}$ parameter in Eqs. (3) and (4) contains sidereal time independent SME coefficients. This term can affect both shape and normalization. We note that each of these two models considers disappearance in only one channel while the complete formula [Eq. (2)] contains contributions from both. However, the limits reported tend to be more conservative than if both channels were considered simultaneously.

The SME parameters in Eqs. (3) and (4) are extracted using the MC expectation and background subtracted data (Fig. 1), the total error matrix including statistical and correlated systematic contributions, and a least squares fitting technique. The least squares estimator is minimized in order to find the best fit (BF) among the parameter combinations.

The e-τ and e-μ BF sidereal time results are shown in Fig. 2. The BF results for both fits are dominated by the sidereal time independent terms, $(\mathcal{C})_{\bar{e}\bar{\tau}}$ and $(\mathcal{C})_{\bar{e}\bar{\mu}}$. We examine the significance of the results below.

The flatness of the sidereal time distribution is analyzed using a frequentist approach. A large sample of randomized pseudoexperiments based on the MC expectation and the total error matrix and with an injected sidereal time independent ("flat") disappearance is generated in order to determine the fraction of samples that present a more or less flat solution than the one found here. We introduce a normalization factor of 91.8%, consistent with the
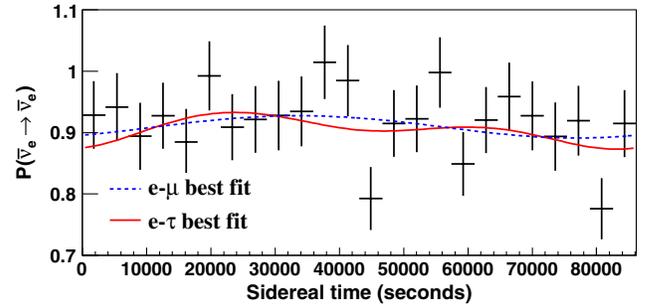

FIG. 2 (color online). The electron antineutrino disappearance probability as a function of sidereal time overlaid with the best fit e-μ ($\chi^2/\text{ndf} = 28.8/21$) and e-τ ($\chi^2/\text{ndf} = 27.7/19$) curves. A one parameter flat fit to the distribution yields a best fit with $\chi^2/\text{ndf} = 30.6/23$.

counting-only disappearance probability, in order to ensure that we are testing the null hypothesis that there is no sidereal time dependence rather than the null hypothesis that there is no antineutrino disappearance. The $\Delta\chi^2$ is defined as the minimum χ^2 from the flat hypothesis minus the minimum χ^2 from each e-τ or e-μ fit. This frequentist study shows that 60.0% (41.8%) of pseudoexperiments have a larger $\Delta\chi^2$ than the real data and that the e-τ (e-μ) results are consistent with sidereal time independent oscillations. In the absence of a sidereal dependence, we proceed to set limits on the relevant time dependent SME coefficients. Limits on the SME coefficients and allowed regions around the BF parameters are determined by constructing a five- and three-dimensional parameter space, corresponding to the e-τ and e-μ fits, respectively. By assuming the minimum of the least squares fit estimator follows a χ^2 distribution, a 68% C.L. (95% C.L.) hypervolume can be defined as the region enclosed by the constant χ^2 hypersurface with minimum χ^2 plus 5.9 (11.3) for the e-τ fit, and 3.5 (8.0) for the e-μ fit. These criteria are tested by using a sample of pseudoexperiments with an injected signal based on the BF. That is, each pseudoexperiment sample is convolved with the BF oscillation probability equation. A new fit is then performed and the BF parameters are tallied. We find that the above choices for 68% C.L. (95% C.L.) hypersurfaces enclose 70.1% (68.8%) and 94.5% (94.7%) of BF points for the e-τ (e-μ) fits and that our allowed regions are valid. Note that we have considered only half of the parameter space in this procedure and that the sign reversed BF parameters are equally valid.

The results are summarized in Table I. The BF values from both the e-τ and e-μ fits are shown along with 68% C.L. allowed regions and 95% C.L. upper limits, when applicable. The allowed regions are generally asymmetric; however, the larger of the two-sided region is reported. Correlations between parameters and multiple connected solutions make it impossible to extract meaningful allowed regions for the e-τ fit. The combination of SME coefficients associated with each measured parameter

is also shown in the table. All e-τ parameter limits as well as the sidereal time dependent e-μ limits are on the order of $\sim 10^{-20}$ GeV for *CPT*-odd coefficients and $\sim 10^{-17}$ for *CPT*-even coefficients.

Although every measured sidereal time dependent parameter is consistent with zero, the time independent parameter $(\mathcal{C})_{\bar{e}\bar{\mu}}$ is nonzero at the 96% C.L. We note that a normalization-only fit $[P_{\bar{\nu}_e \to \bar{\nu}_e} \simeq 1 - \frac{L^2}{(\hbar c)^2}((\mathcal{C})^2_{\bar{e}\bar{\tau}} + (\mathcal{C})^2_{\bar{e}\bar{\mu}})]$ yields $(\mathcal{C})^2_{\bar{e}\bar{\tau}} + (\mathcal{C})^2_{\bar{e}\bar{\mu}} = (34.2 \pm 9.2) \times 10^{-40}$ GeV^2. This disappearance is consistent with the rate-only θ_{13} measurement in Ref. [2]. With current precision, time independent Lorentz violating effects cannot be distinguished from mass and θ_{13} induced oscillations. Separating the two effects may be possible with future high statistics data and spectral information, however. The disappearance observed can generally be interpreted as due to neutrino mass and θ_{13} in the three flavor neutrino oscillation framework.

There are a number of alternative neutrino oscillation models motivated by Lorentz violation [15–19]. These models neglect sidereal modulations by assuming that any such variations are averaged out or that the probability of oscillation is governed by time independent terms only. The models focus on reproducing the global observed energy and baseline dependence of neutrino oscillations. Interestingly, however, none of the models predict the observed antineutrino oscillations at Double Chooz's energy ($\langle E \rangle = 4.2$ MeV) and baseline (1050 m). That is, the measured disappearance conflicts with these models. This may be an additional reason to interpret the time independent disappearance observed as due to neutrino mass and nonzero θ_{13}, rather than time independent Lorentz violation.

We have analyzed the sidereal time dependence of Double Chooz's electron antineutrino candidates as a probe of Lorentz violation. With no observed modulation, we set the first limits on 14 of the SME coefficients in the e-τ sector, and set competitive limits on two e-μ sector coefficients. Competitive limits may also be provided by other reactor antineutrino experiments in the future [20,21],

TABLE I. A summary of the e-τ and e-μ Lorentz violation measurements in terms of the best fit parameters and the corresponding combinations of Standard-Model Extension coefficients. The allowed regions and limits reported are set by the extremes of the multidimensional confidence regions. The average antineutrino energy E is 4.2×10^{-3} GeV.

	BF parameter $(10^{-20}$ GeV)	Upper limit (95% C.L.)	SME coefficients combination
$(\mathcal{C})_{\bar{e}\bar{\tau}}$	5.8	7.8	$[-(a_L)^T_{e\tau} - 0.29(a_L)^Z_{e\tau}] + E[-1.46(c_L)^{TT}_{e\tau} - 0.57(c_L)^{TZ}_{e\tau} + 0.38(c_L)^{ZZ}_{e\tau}]$
$(\mathcal{A}_s)_{\bar{e}\bar{\tau}}$	-0.4	6.6	$[-0.91(a_L)^X_{e\tau} + 0.29(a_L)^Y_{e\tau}] + E[-1.83(c_L)^{TX}_{e\tau} + 0.58(c_L)^{TY}_{e\tau} - 0.52(c_L)^{XZ}_{e\tau} + 0.16(c_L)^{YZ}_{e\tau}]$
$(\mathcal{A}_c)_{\bar{e}\bar{\tau}}$	0.4	7.0	$[0.29(a_L)^X_{e\tau} + 0.91(a_L)^Y_{e\tau}] + E[0.58(c_L)^{TX}_{e\tau} + 1.83(c_L)^{TY}_{e\tau} + 0.16(c_L)^{XZ}_{e\tau} + 0.52(c_L)^{YZ}_{e\tau}]$
$(\mathcal{B}_s)_{\bar{e}\bar{\tau}}$	0.0	5.4	$E[0.26((c_L)^{XX}_{e\tau} - (c_L)^{YY}_{e\tau}) + 0.75(c_L)^{XY}_{e\tau}]$
$(\mathcal{B}_c)_{\bar{e}\bar{\tau}}$	0.5	5.4	$E[0.38((c_L)^{XX}_{e\tau} - (c_L)^{YY}_{e\tau}) - 0.53(c_L)^{XY}_{e\tau}]$
$(\mathcal{C})_{\bar{e}\bar{\mu}}$	5.8 ± 1.7	$\cdots$	$[-(a_L)^T_{e\mu} - 0.29(a_L)^Z_{e\mu}]$
$(\mathcal{A}_s)_{\bar{e}\bar{\mu}}$	-0.4 ± 0.7	1.9	$[-0.91(a_L)^X_{e\mu} + 0.29(a_L)^Y_{e\mu}]$
$(\mathcal{A}_c)_{\bar{e}\bar{\mu}}$	0.5 ± 0.8	5.5	$[0.29(a_L)^X_{e\mu} + 0.91(a_L)^Y_{e\mu}]$

although Double Chooz features a comparatively simple antineutrino-source-to-detector vector. With the addition of this work amongst the world's data, sidereal variation tests with neutrino oscillation experiments have been performed with all active oscillation channels. In the future, astrophysical neutrinos [22] may improve sensitivity to Lorentz violation by many orders of magnitude compared to what is possible for terrestrial neutrino experiments.

[1] Y. Abe *et al.*, Phys. Rev. Lett. **108**, 131801 (2012).
[2] Y. Abe *et al.*, Phys. Rev. D **86**, 052008 (2012).
[3] V. A. Kostelecký and S. Samuel, Phys. Rev. D **39**, 683 (1989).
[4] P. Adamson *et al.*, Phys. Rev. Lett. **101**, 151601 (2008); **105**, 151601 (2010); Phys. Rev. D **85**, 031101 (2012).
[5] R. Abbasi *et al.*, Phys. Rev. D **82**, 112003 (2010).
[6] L. B. Auerbach *et al.*, Phys. Rev. D **72**, 076004 (2005).
[7] A. A. Aguilar-Arevalo *et al.*, arXiv:1109.3480.
[8] D. Colladay and V. A. Kostelecký, Phys. Rev. D **55**, 6760 (1997); **58**, 116002 (1998); V. A. Kostelecký, Phys. Rev. D **69**, 105009 (2004).
[9] V. A. Kostelecký and M. Mewes, Phys. Rev. D **69**, 016005 (2004).
[10] C. L. Jones, A. Bernstein, J. M. Conrad, Z. Djurcic, M. Fallot, L. Giot, G. Keefer, A. Onillon, and L. Winslow, Phys. Rev. D **86**, 012001 (2012).

[11] P. Huber, Phys. Rev. C **84**, 024617 (2011).
[12] T. A. Mueller *et al.*, Phys. Rev. C **83**, 054615 (2011).
[13] Y. Declais *et al.*, Phys. Lett. B **338**, 383 (1994).
[14] V. A. Kostelecký and M. Mewes, Phys. Rev. D **70**, 076002 (2004).
[15] V. A. Kostelecký and M. Mewes, Phys. Rev. D **70**, 031902 (2004).
[16] T. Katori, V. A. Kostelecký, and R. Tayloe, Phys. Rev. D **74**, 105009 (2006).
[17] V. Barger, J. Liao, D. Marfatia, and K. Whisnant, Phys. Rev. D **84**, 056014 (2011).
[18] J. S. Díaz and V. A. Kostelecký, Phys. Lett. B **700**, 25 (2011).
[19] J. S. Díaz and V. A. Kostelecký, Phys. Rev. D **85**, 016013 (2012).
[20] F. P. An *et al.*, Phys. Rev. Lett. **108**, 171803 (2012).
[21] J. K. Ahn *et al.*, Phys. Rev. Lett. **108**, 191802 (2012).
[22] R. Abbasi *et al.*, Nature (London) **484**, 351 (2012).